Supplementary materials

Correlation between small earthquakes and CO_2 anomalies in spring waters: a statistical experiment on the probability of seismic occurrence

C. Fidani [1,2], F. Gherardi [3*], G. Facca [3], L. Pierotti [3]

[1] Istituto Nazionale di Geofisica e Vulcanologia, Roma, Italy

[2] Central Italy Electromagnetic Network, Fermo, Italy

[3] Istituto di Geoscienze e Georisorse CNR, Pisa, Italy

*** Correspondence to:** f.gherardi@igg.cnr.it

1. **The irregular component of the 61 CO_2 anomalies detected by the Gallicano station in Tuscany, Italy, from April 2017 to March 2021**

For the decomposition of the CO_2 series, we applied the CENSUS method, with the STATISTICA® 7.0 software (Statsof Inc., 2005). The CENSUS technique (Makridakis et al.,1998) is a method to decompose a time series in four different components: (1) seasonal component (denoted as St, where t stands for the particular point in time); (2) trend component (Tt); (3) cyclical component (Ct); and (4) random error, or irregular component (It). The difference between a cyclical and a seasonal component is that the latter occurs at regular (seasonal) intervals, while cyclical factors have usually a longer duration that varies from cycle to cycle. In the CENSUS I method, the trend and cyclical components are customarily combined into a trend-cycle component (TCt). The specific functional relationship between these components can assume different forms. However, two straightforward possibilities are that they combine according to an additive (Xt = TCt+St+It) or a (Xt = Tt×Ct×St×It) multiplicative model. The additive model is applied when the seasonal fluctuations of the recorded geochemical signal are steady, and not dependent on the overall level of the series.

The decomposition is performed following a step-by-step procedure: (i) determination of the duration of one season. In this study we consider a reference frame of 12 months, by exploring the effects (always negligible in our case study) of different setup with seasons of 4 and 3 months; (ii) computation of the centered moving average of the series, with a window width of one season; (iii) computation of the seasonal component (St) by subtracting the moving average from the original dataset; (iv) computation of the so-called ‘‘seasonally adjusted series’’ by removing the seasonal component from original series; (v) individuation of the trend/cycle component (TCt), by smoothing the seasonally adjusted series; (vi) calculation of the irregular component by subtracting the seasonal and trend/cycle components from the original data series.

The 61 value of the CO_2 irregular component are reported in Table SM1.

Table SM1. CO_2 irregular component.

Time	Irregular component	Anomalies
10/04/2017	-0.104474787	1
09/05/2017	-0.090324244	1
10/05/2017	0.082259825	1
18/05/2017	0.120264997	1
24/05/2017	-0.086884028	1
25/05/2017	0.092515372	1
30/05/2017	0.106715525	1
31/05/2017	0.169639702	1
01/06/2017	-0.357154105	1
03/06/2017	0.076612614	1
08/06/2017	-0.094938563	1
09/08/2017	-0.077010804	1
22/10/2017	0.074178579	1
04/04/2018	0.082900366	1
05/04/2018	-0.086713431	1
26/06/2018	-0.088605383	1
28/06/2018	0.083642797	1
23/09/2018	0.08581652	1
05/10/2018	-0.083109269	1
26/10/2018	0.092079309	1
31/01/2019	0.075470479	1
01/02/2019	0.095814993	1
02/02/2019	-0.205264112	1
17/04/2019	0.084024524	1
11/06/2019	0.083594834	1
12/06/2019	0.205989943	1
13/06/2019	-0.533256804	1
14/06/2019	0.152195777	1
15/06/2019	0.088933257	1
09/07/2019	0.103048376	1
16/07/2019	-0.141104497	1
17/07/2019	0.169573217	1
18/07/2019	-0.128874368	1
19/07/2019	-0.074913529	1
21/07/2019	-0.096577061	1

22/07/2019	0.26352478	1
24/07/2019	-0.329618998	1
25/07/2019	0.200411251	1
26/07/2019	0.084738512	1
10/09/2019	0.08746406	1
11/09/2019	-0.098343389	1
05/11/2019	0.124189652	1
06/11/2019	-0.108796658	1
07/11/2019	-0.091348563	1
25/11/2019	-0.083329587	1
12/05/2020	0.094858987	1
05/06/2020	-0.115311196	1
31/10/2020	0.175799952	1
01/11/2020	-0.205439467	1
19/11/2020	-0.274940171	1
21/11/2020	0.191572574	1
02/12/2020	0.211414361	1
03/12/2020	-0.08232999	1
04/12/2020	-0.111501103	1
06/12/2020	-0.090378058	1
11/12/2020	-0.111300715	1
12/12/2020	0.180359739	1
17/12/2020	-0.278440233	1
18/12/2020	0.081573768	1
19/12/2020	0.150362996	1
02/01/2021	-0.09448945	1

We tested the stability of the irregular component by exploring the effects induced by the application of a random component to input data. In particular, we introduced a random noise of 2%, of the same magnitude of the maximum instrumental error. Then, we applied the Census I method to this new irregular component. The robustness of the procedure was finally evaluated by comparing the new synthetic signal with the initial one. Figure SM1 shows that the procedure produced almost the same number of significant peaks both in the original and synthetic cases.

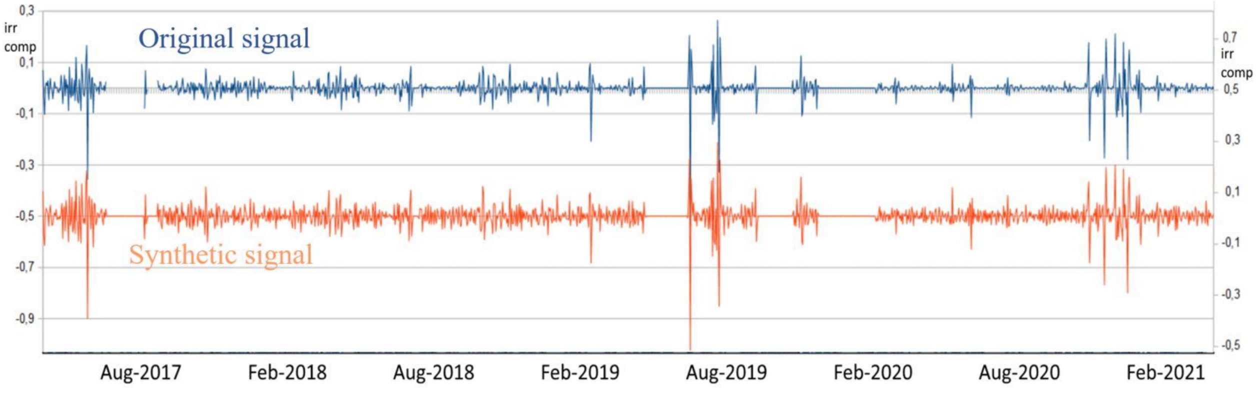

Figure SM1. Comparison between the original irregular component (“Original signal”) and the irregular component obtained after adding a 2% of random noise to the CO_2 signal (“Synthetic signal”). In the new irregular component, we notice an increase of the noise. However, most of the anomalies are still evident, with only 5% of them disappeared after introduction of the random noise.

The new distribution closely approaches a Gaussian distribution. We observed the same major peaks with the same time lag, and values above the fluctuation levels for each model. Specifically, only three anomalies disappeared (February 2018, October 2018 and April 2019).

2. Mainshocks around the station of Gallicano in Tuscany, Italy, from April 2017 to March 2021

We applied the zmap software of Matlab version 7.1, which loaded the "INGV_fdsn" database with 3402 events, from 2017-03-09T15:19:34.670000 to 2021-04-18T19:28:21.210000. The selected area covered a radius of 50 km around the Gallicano spring (longitude interval from 9.8198° to 11.1258°N; latitude interval from 43.5668° to 44.5377°E), with depths comprised between 0.1 to 50 km b.g.l.. The local magnitude ranged between 0.4 and 3.6. We used the Reasemberg (1985) and Gardner & Knopoff (1974) declustering options to obtain a preliminary set of 785 seismic events, that were further reduced to 71, by applying distance-to-magnitude selection criteria discussed in the main text. This step was proved to be roughly equivalent to selecting only seismic events occurred within three (3) Dobrovolsky radii (Dobrovolsky et al., 1979) from the Gallicano spring. Finally, by considering a maximum of one seismic event per day (see main text for further details), we were able to single out a total of 42 main shocks (Table SM2).

Table SM2. Times, coordinates, depths, and magnitudes of the 44 seismic events correlated with the 61 CO_2 anomalies. The column 8 reports the distance between the Gallicano spring and the earthquake epicentre. Columns 1 and 7 report the event number and the location name, respectively. The column 9 reports the Dobrovolsky radius correspondent to the seismic magnitude.

#EventID	Time	Latitude N	Longitude E	Depth/Km	Magnitude	Event Location Name	distIp	distDobr	Ip<3Dobr
14430851	26/03/2017	44.0923	10.4295	11.4	1.6	2 km NE Molazzana (LU)	11.97645282	4.87528490	1
14486011	29/03/2017	44.1223	10.7377	11.5	2.5	3 km NW Cutigliano (PT)	27.66113568	11.8850223	1
15082961	01/05/2017	44.2442	10.3667	8.1	2.4	6 km E Sillano Giuncugnano (LU)	22.70899519	10.7646521	1
15273541	11/05/2017	44.258	10.7282	19.6	2.4	1 km NE Montecreto (MO)	37.65668482	10.7646521	1
15799041	09/06/2017	44.2197	10.0648	10.4	2.8	5 km W Fivizzano (MS)	36.0054975	15.9955803	1
17131831	22/09/2017	44.1447	10.4792	8.6	2	4 km NE Fosciandora (LU)	13.26844688	7.2443596	1
17166551	26/09/2017	44.2473	10.7617	10.3	2.9	2 km NW Sestola (MO)	34.94765952	17.6603782	1
17436871	24/10/2017	44.0378	10.2697	5.7	2	5 km NW Stazzema (LU)	14.55562626	7.2443596	1
17579161	06/11/2017	44.2328	10.7757	7.9	3.1	Sestola (MO)	34.24417027	21.5278173	1
17914711	24/12/2017	44.1923	10.2027	8.4	2.5	2 km E Casola in Lunigiana (MS)	25.12157091	11.8850223	1
17997381	07/01/2018	44.1008	10.7908	11.7	2.5	3 km E Cutigliano (PT)	31.0639872	11.8850223	1
18155041	31/01/2018	43.9463	10.3002	4.7	2	1 km NW Camaiore (LU)	17.18204735	7.2443596	1
18300711	22/02/2018	44.4238	10.3633	22.5	3.3	4 km W Castelnovo ne' Monti (RE)	46.63087213	26.2421854	1
18429141	12/03/2018	44.1235	10.415	7.5	1.4	1 km S Pieve Fosciana (LU)	10.45441294	3.9994475	1
18974251	23/04/2018	44.1328	10.4158	9.8	1.9	Pieve Fosciana (LU)	12.8308614	6.56145266	1
19218021	07/05/2018	44.0442	10.2717	7.5	2.1	6 km NW Stazzema (LU)	15.11741685	7.99834255	1
19876281	28/06/2018	44.2148	10.5832	13.9	2.2	3 km W Pievepelago (MO)	25.1153739	8.830799	1
19911391	01/07/2018	44.1803	10.548	14.2	3.6	6 km W Pievepelago (MO)	21.5214303	35.318317	1
20146301	24/07/2018	44.2072	10.552	16.4	2.3	5 km W Pievepelago (MO)	25.00767187	9.74989638	1
20761101	25/09/2018	44.0752	10.4112	8	1.2	1 km W Molazzana (LU)	8.402745264	3.28095293	1
21404131	22/01/2019	44.1608	10.6223	7.9	2.4	3 km SW Fiumalbo (MO)	20.31801299	10.7646521	1
22328081	25/05/2019	44.1148	10.4093	8	1.6	Castelnuovo di Garfagnana (LU)	10.29033329	4.8752849	1
22408201	07/06/2019	43.9837	10.1472	9.9	3.2	3 km NW Forte dei Marmi (LU)	26.37176198	23.7684029	1
22635331	08/07/2019	44.3697	10.4747	9.1	2.7	1 km NE Villa Minozzo (RE)	35.76173272	14.4877185	1
22861481	14/08/2019	44.3897	10.6112	9.4	2.7	3 km NW Montefiorino (MO)	40.3767534	14.4877185	1
23137951	22/09/2019	43.9377	10.2918	5.2	2.9	1 km W Camaiore (LU)	18.43673551	17.6603782	1
23324101	25/10/2019	43.9332	10.2957	6.1	2.5	1 km SW Camaiore (LU)	18.8898624	11.8850223	1
23582511	12/12/2019	44.1235	10.4182	7.6	1.9	1 km SE Pieve Fosciana (LU)	10.49107207	6.56145266	1
23801501	21/01/2020	44.0983	10.7262	14.3	3	2 km W Cutigliano (PT)	27.6366558	19.498446	1
24086211	10/03/2020	43.939	10.31	6	2.6	Camaiore (LU)	17.71874533	13.121999	1
24124341	20/03/2020	43.9412	10.3103	5.4	2	Camaiore (LU)	17.32533931	7.2443596	1
24187771	31/03/2020	44.2887	10.2307	20.6	2.9	8 km E Comano (MS)	36.56768126	17.6603782	1
24418031	14/05/2020	44.2487	10.5223	11.1	2.7	7 km SW Frassinoro (MO)	24.76363682	14.4877185	1
24620611	11/06/2020	44.3327	10.5752	8.9	3.1	4 km N Frassinoro (MO)	33.53616463	21.5278173	1
24745491	30/06/2020	44.3162	10.7013	20.3	2.8	3 km W Lama Mocogno (MO)	40.94552281	15.9955803	1
25139151	26/08/2020	44.2085	10.6528	11.1	2.7	3 km S Riolunato (MO)	26.44880155	14.4877185	1
25769171	07/12/2020	44.2028	10.2113	6.8	3.1	3 km E Casola in Lunigiana (MS)	24.85062096	21.5278173	1
25790911	14/12/2020	44.1232	10.4187	7.1	1.8	1 km SE Pieve Fosciana (LU)	10.10623693	5.94292159	1
25915491	11/01/2021	44.1735	10.6838	13	2.6	3 km E Fiumalbo (MO)	26.90831362	13.121999	1
26086241	13/02/2021	44.1277	10.4192	7.7	1.9	1 km SE Pieve Fosciana (LU)	10.87353216	6.56145266	1
26369691	02/04/2021	44.139	10.4082	7.9	1.6	1 km NW Pieve Fosciana (LU)	12.03698226	4.8752849	1
26473861	18/04/2021	44.1285	10.6197	11.9	2.5	4 km W Abetone (PT)	20.44608504	11.8850223	1

3. Strong seismic events occurred in the world, in the Mediterranean area, and in Italy, from April 2017 to March 2021

We further inspected our time series to exclude any hypothetical correlation between CO_2 anomalies and major earthquakes occurred worldwide during the observation period (passage of Rayleigh seismic waves; e.g., Manga and Wang, 2015). This test was done for further caution, considered that (i) the influence of major earthquakes has been documented in the literature only for variations in groundwater levels/pressure (e.g., Cooper et al., 1965; Brodsky et al., 2003; Sil et al., 2006; Shi and Wang, 2014; Zhang et al., 2015; He et al., 2020; Barberio et al., 2020), not CO_2 concentrations, and (ii) that variations in fluid pressure are not necessarily correlated to variations in CO_2 concentration.
This assessment was based on the lack of correlation with Italian, Mediterranean, and global earthquakes with magnitude greater than or equal to 4.5, 5.5 and 6.5, respectively. Global seismic events of magnitude ≥ 6.5 are reported in Table SM3, Mediterranean seismic events of magnitude ≥ 5.5 are reported in Table SM4, and Italian seismic events of magnitude ≥ 4.5 are reported in Table SM5.
Overall, no coincidence was identified between the passage of the Rayleigh waves and CO_2 anomalies at Gallicano.

Table SM3. Times, coordinates, depths, and magnitudes of the 148 seismic events with M ≥ 6.5 recorded in the world from April 2017 to March 2021. Retrieved from USGS.

Time	Latitude N	Longitude E	Depth/Km	Magnitude
2017-04-24	-33.0375	-72.0617	28	6.9
2017-04-28	5.5043	125.0658	26	6.9
2017-05-09	-14.5884	167.3767	169	6.8
2017-05-10	-56.414	-25.7432	15	6.5
2017-05-29	-1.2923	120.4313	12	6.6
2017-06-02	54.0312	170.9196	5	6.8
2017-06-14	14.9091	-92.0092	93	6.9
2017-06-22	13.7174	-90.9718	38	6.8
2017-07-06	11.1269	124.6286	9	6.5
2017-07-11	-49.4837	164.0157	10	6.6
2017-07-17	54.4434	168.857	10	7.7
2017-07-20	36.9293	27.4139	7	6.6
2017-08-08	33.1926	103.8552	9	6.5
2017-08-18	-1.112	-13.6605	35	6.6
2017-09-08	15.0222	-93.8993	47	8.2
2017-09-19	18.5499	-98.4887	48	7.1
2017-10-08	52.3909	176.7691	119	6.5
2017-10-10	-54.2632	8.6086	9	6.7
2017-10-24	-7.2168	123.0735	553	6.7
2017-10-31	-21.6971	169.1485	24	6.7
2017-11-01	-21.6484	168.8585	22	6.6
2017-11-04	-15.3197	-173.1682	10	6.8
2017-11-07	-4.2433	143.4846	110	6.5
2017-11-12	34.9109	45.9592	19	7.3
2017-11-13	9.5147	-84.4865	19	6.5
2017-11-19	-21.5027	168.5984	13	6.6
2017-11-19	-21.3246	168.6715	10	7
2017-11-30	-1.0802	-23.4323	10	6.5
2017-12-13	-54.2189	2.1628	17	6.5
2017-12-15	-7.4921	108.1743	90	6.5
2018-01-10	17.4825	-83.52	19	7.5
2018-01-14	-15.7675	-74.7092	39	7.1
2018-01-23	56.0039	-149.1658	14	7.9
2018-01-28	-53.0623	9.6842	10	6.6
2018-02-16	16.3855	-97.9787	22	7.2
2018-02-25	-6.0699	142.7536	25	7.5

2018-03-06	-6.3043	142.6116	20	6.7
2018-03-08	-4.3762	153.1996	22	6.8
2018-03-26	-5.5024	151.4025	40	6.7
2018-03-29	-5.5321	151.4999	35	6.9
2018-04-02	-20.6588	-63.0058	559	6.8
2018-05-04	19.3181	-154.9996	5.8	6.9
2018-08-05	-8.2581	116.4375	34	6.9
2018-08-15	51.4234	-178.0262	33	6.5
2018-08-17	-7.3718	119.8017	529	6.5
2018-08-19	-18.1125	-178.153	600	8.2
2018-08-19	-8.319	116.6272	21	6.9
2018-08-21	10.7731	-62.9019	146	7.3
2018-08-21	-16.0315	168.1428	9	6.5
2018-08-24	-11.0355	-70.8284	630	7.1
2018-08-29	-22.0295	170.1262	21	7.1
2018-09-05	42.6861	141.9294	35	6.6
2018-09-06	-18.4743	179.3502	670	7.9
2018-09-09	-10.0207	161.5025	68	6.5
2018-09-10	-31.7447	-179.3728	115	6.9
2018-09-16	-25.415	178.1991	576	6.5
2018-09-28	-0.2559	119.8462	20	7.5
2018-09-30	-18.3604	-178.0633	550	6.7
2018-10-10	-5.7012	151.2046	39	7
2018-10-10	49.2902	156.2968	20	6.5
2018-10-13	52.8549	153.2429	461	6.7
2018-10-16	-21.7427	169.5217	17	6.5
2018-10-22	49.2586	-129.4124	10	6.5
2018-10-22	49.3346	-129.289	10	6.8
2018-10-22	49.297	-129.7237	10	6.5
2018-10-25	37.5203	20.5565	14	6.8
2018-11-09	71.6312	-11.2431	10	6.7
2018-11-18	-17.8735	-178.9273	540	6.8
2018-11-30	61.3464	-149.9552	46.7	7.1
2018-12-05	-21.9496	169.4266	10	7.5
2018-12-05	-22.0629	169.7331	10	6.6
2018-12-11	-58.5446	-26.3856	133	7.1
2018-12-20	55.0999	164.6993	16.5	7.3
2018-12-29	5.8983	126.9209	60.2	7
2019-01-05	-8.144	-71.587	570	6.8
2019-01-06	2.258	126.758	43.2	6.6
2019-01-15	-13.336	166.8752	35	6.6
2019-01-20	-30.0404	-71.3815	63	6.7
2019-01-22	-43.1219	42.3568	13	6.7
2019-02-01	14.6802	-92.4527	66	6.7
2019-02-22	-2.1862	-77.0505	145	7.5
2019-03-01	-14.7131	-70.1546	267	7
2019-04-09	-58.6262	-25.304	38	6.5
2019-04-12	-1.8146	122.5798	15.4	6.8
2019-05-06	-6.9746	146.4494	146	7.1
2019-05-14	-4.051	152.5967	10	7.6
2019-05-26	-5.8119	-75.2697	122	8
2019-05-30	13.1994	-89.3056	57.9	6.6
2019-06-15	-30.6441	-178.0995	46	7.3
2019-06-24	-6.4078	129.1692	212	7.3
2019-07-06	35.7695	-117.5993	8	7.1
2019-07-07	0.5126	126.1892	35	6.9
2019-07-14	-18.2242	120.3584	10	6.6
2019-07-14	-0.5858	128.034	18.9	7.2
2019-07-31	-16.1985	167.9982	181	6.6

2019-08-01	-34.2364	-72.3102	25	6.8
2019-08-02	-7.2822	104.7907	49	6.9
2019-08-27	-60.2152	-26.5801	16	6.6
2019-09-01	-20.3641	-178.5701	591	6.6
2019-09-25	-3.4528	128.3699	12.2	6.5
2019-09-29	-35.4758	-73.163	11	6.7
2019-10-29	6.7567	125.0082	15	6.6
2019-10-31	6.9098	125.1782	10	6.5
2019-11-04	-18.5747	-175.272	10	6.6
2019-11-08	-21.9449	-179.5113	577	6.5
2019-11-14	1.6213	126.4156	33	7.1
2019-12-15	6.6969	125.1739	18	6.8
2020-01-24	38.4312	39.0609	10	6.7
2020-01-28	19.4193	-78.756	14.8	7.7
2020-02-13	45.6161	148.959	143	7
2020-03-25	48.9638	157.6955	57.8	7.5
2020-03-31	44.4646	-115.1175	12.1	6.5
2020-04-18	27.1264	140.1349	453	6.6
2020-05-02	34.1818	25.7101	10	6.5
2020-05-06	-6.7761	129.7852	96	6.8
2020-05-12	-12.0665	166.6485	107	6.6
2020-05-15	38.1689	-117.8497	2.7	6.5
2020-06-03	-23.274	-68.4677	112	6.8
2020-06-13	28.8591	128.2713	165	6.6
2020-06-18	-33.2927	-177.8571	10	7.4
2020-06-23	15.8861	-96.0077	20	7.4
2020-07-06	-5.6023	110.6893	533	6.6
2020-07-17	-7.836	147.7704	73	7
2020-07-22	55.0715	-158.596	28	7.8
2020-08-18	12.0257	124.1272	10	6.6
2020-08-18	-4.3217	101.1347	22	6.8
2020-08-18	-4.2069	101.2411	26	6.9
2020-08-21	-6.71	123.4649	624	6.9
2020-08-30	0.7821	-29.8656	10	6.5
2020-09-01	-27.9686	-71.3062	21	6.8
2020-09-01	-27.9162	-71.3701	16	6.5
2020-09-06	7.6829	-37.1544	10	6.7
2020-09-18	0.9298	-26.8533	10	6.9
2020-10-19	54.602	-159.6258	28	7.6
2020-10-30	37.8973	26.7838	21	7
2020-12-27	-39.3398	-74.9849	10	6.7
2021-01-11	51.2811	100.4383	10	6.7
2021-01-21	4.9931	127.5145	80	7
2021-01-23	-61.8098	-55.5027	15	6.9
2021-02-03	-36.2797	-97.8	10	6.7
2021-02-10	-23.0511	171.6566	10	7.7
2021-02-13	37.7265	141.7751	43	7.1
2021-03-04	-37.4787	179.4576	10	7.3
2021-03-04	-29.6768	-177.8398	43	7.4
2021-03-04	-29.7228	-177.2794	28	8.1
2021-03-04	-28.5168	-176.6801	24	6.5
2021-03-16	54.7368	163.1803	13	6.6
2021-03-20	38.4515	141.6477	43	7

Table SM4. Times, coordinates, depths, and magnitudes of the 31 seismic events with M ≥ 5.5 recorded in the Mediterranean area from April 2017 to March 2021. Retrieved from USGS.

Time	Latitude N	Longitude E	Depth/Km	Magnitude	Event location name
6/12/2017	38.9296	26.365	12	6.3	5 km S of Plomari, Greece
7/20/2017	36.9293	27.4139	7	6.6	11 km ENE of Kos, Greece
6/25/2018	36.6404	21.3431	10	5.5	37 km WSW of Methani, Greece
10/25/2018	37.5203	20.5565	14	6.8	32 km SW of Lithakia, Greece
10/28/2018	45.6575	26.3972	151	5.5	15 km SE of Comandău, Romania
10/30/2018	37.5124	20.5076	11	5.7	36 km SW of Lithakia, Greece
3/20/2019	37.4078	29.531	8	5.7	16 km E of Acipayam, Turkey
8/8/2019	37.935	29.7003	11	5.9	9 km ESE of Baklan, Turkey
9/21/2019	41.3375	19.5303	20	5.6	3 km WSW of Shijak, Albania
9/26/2019	40.9035	28.1502	8	5.7	17 km ESE of Marmara Ereğlisi, Turkey
11/26/2019	41.5138	19.5256	22	6.4	15 km WSW of Mamurras, Albania
11/26/2019	41.5708	19.4242	10	5.5	22 km W of Mamurras, Albania
11/27/2019	35.7174	23.2284	69	6	45 km WNW of Kissamos, Greece
1/22/2020	39.0724	27.8389	5.6	5.6	15 km ESE of Kirkağaç, Turkey
1/28/2020	35.2183	27.8918	10	5.5	69 km ESE of Karpathos, Greece
1/30/2020	35.1565	27.8845	10	5.5	72 km ESE of Karpathos, Greece
1/30/2020	35.1817	27.7814	10	5.7	63 km SE of Karpathos, Greece
3/21/2020	39.3567	20.6383	10	5.7	38 km SSW of Giannina, Greece
5/2/2020	34.1818	25.7101	10	6.5	91 km S of Ierapetra, Greece
5/18/2020	34.1855	25.5173	10	5.7	92 km S of Ierapetra, Greece
5/20/2020	35.1594	20.2775	13.45	5.7	224 km SW of Methoni, Greece
9/18/2020	35.0368	25.3034	44	5.9	12 km SSE of Arkalochori, Greece
10/30/2020	37.8973	26.7838	21	7	10 km NNE of Agios Konstantinos, Greece
12/29/2020	45.4244	16.2573	10	6.4	2 km WSW of Petrinja, Croatia
2/17/2021	38.4057	22.019	5.29	5.5	11 km N of Kamárai, Greece
3/3/2021	39.7546	22.1757	8	6.3	9 km W of Tirnavos, Greece
3/4/2021	39.7865	22.1157	10	5.8	11 km E of Verdikousa, Greece
3/4/2021	39.8812	21.9795	10	5.5	7 km S of Krania Elassonos, Greece
3/12/2021	39.8931	22.0875	7	5.6	8 km W of Elassona, Greece
3/18/2021	36.9206	5.2014	8	6	21 km NNE of Béjaïa, Algeria
3/27/2021	42.4479	16.0496	7	5.5	55 km N of Peschici, Italy

Table SM5. Times, coordinates, depths, and magnitudes of the 50 seismic events with M ≥ 4.5 recorded in the Italian territory from April 2017 to March 2021. Retrieved from INGV.

#EventID	Time	Latitude	Longitude	Depth/Km	Magnitude Type	Magnitude
14662201	4/8/2017	41.7542	19.9353	19.8	mb	5.1
14818711	4/15/2017	36.2197	18.8064	10.0	mb	4.5
17979171	1/4/2018	42619	19.8865	10.1	mb	5.2
18181591	2/3/2018	43.3178	16853	19.7	mb	4.8
18387591	3/8/2018	36.9352	10.2568	19.5	mb	4.7
18673351	4/10/2018	43.0687	13.0365	8.1	Mw	4.6
19950851	7/4/2018	41.4475	19563	14.6	mb	5.1
20362671	8/14/2018	41.8877	14.8407	19.2	Mw	4.6
20375681	8/16/2018	41.8742	14.8648	19.6	Mw	5.1
20415201	8/19/2018	39349	13.3662	525.7	ML	4.6
20533641	8/30/2018	44.0402	16.5674	9.8	mb	4.8

20845861	10/6/2018	37.6088	14.9395	4.5	Mw	4.6
21285011	12/26/2018	37644	15116	-0.3	Mw	4.9
22666191	7/13/2019	37.3008	5.68652	19.5	mb	5.0
23128121	9/21/2019	41.3458	19.4977	17.3	ML	5.4
23128421	9/21/2019	41.3365	19501	28.8	ML	5.2
23487611	11/26/2019	41.3998	19.5207	22.1	Mw	6.2
23492121	11/26/2019	41.4	19.54	10.0	mb	5.1
23489371	11/26/2019	41.49	19.53	10.0	mb	5.3
23490711	11/26/2019	41.5355	19.4663	20.2	ML	5.4
23491021	11/26/2019	41.5093	19.4613	18.0	ML	4.8
23492041	11/26/2019	43.1631	17981	10.4	mb	5.3
23493291	11/26/2019	41.5745	19.6755	36.0	ML	4.7
23494781	11/26/2019	41.5198	19.4773	21.3	ML	4.6
23501081	11/27/2019	41.5643	19.5197	25.0	ML	5.4
23506081	11/28/2019	41.4478	19.3925	14.4	ML	4.8
23558121	12/9/2019	44.0047	11.3192	7.3	Mw	4.5
23621271	12/19/2019	41.3982	19.5679	10.0	mb	4.7
23812111	1/24/2020	36.7488	5.58545	9.8	mb	5.0
23837301	1/28/2020	41.4738	19.4971	12.9	mb	5.0
24134961	3/22/2020	45.8517	15946	10.1	Mw	5.1
24136051	3/22/2020	45.8754	15.9717	9.8	mb	4.9
24163051	3/26/2020	35.7258	5.66895	19.5	mb	5.0
24415521	5/13/2020	35.21	15.24	10.0	mb	4.6
24994741	8/7/2020	36.4605	6.26221	9.8	mb	4.8
24997031	8/7/2020	36.6539	6.33691	19.5	mb	4.7
25307851	9/20/2020	44.2169	15.9387	10.1	mb	4.5
25597961	11/1/2020	44.3325	15504	11.7	ML	4.8
25711191	11/22/2020	36.7506	6.71748	10.4	mb	5.1
25850901	12/28/2020	45.3965	16.2398	8.8	ML	5.2
25851471	12/28/2020	45.3725	16.2218	10.6	ML	4.8
25870121	12/29/2020	45.4033	16.2017	9.1	Mw	6.3
25873821	12/30/2020	45.4157	16.1575	5.7	ML	5.0
25874141	12/30/2020	45.4038	16.1598	8.2	ML	4.8
25903371	1/6/2021	45.3862	16.2213	16.2	ML	5.2
25912621	1/9/2021	45.3542	16.3093	8.5	ML	4.7
26258141	3/18/2021	37023	5.18115	12.9	Mwp	6.2
26258591	3/18/2021	37.0178	5.24048	10.0	mb	5.3
26321911	3/27/2021	42.6728	16.3293	11.1	Mw	5.2

4. Additional sensitivity analysis

We verified the robustness of the correlations shown in the main text (histogram of Figure 4), by exploring the effect of different Δt lag values. In particular, the histogram of Figure SM2 shows that the only relevant CO_2-EQ correlation peak predicted under Δt lag = ±30 days conditions occurs at -2 days, exactly as predicted under Δt lag = ±20 days conditions (condition discussed in the main text). Furthermore, under the Δt lag condition of ±30 days, we did not even notice any significant correlation peak for the Rain-EQ and Rain-CO_2 series.

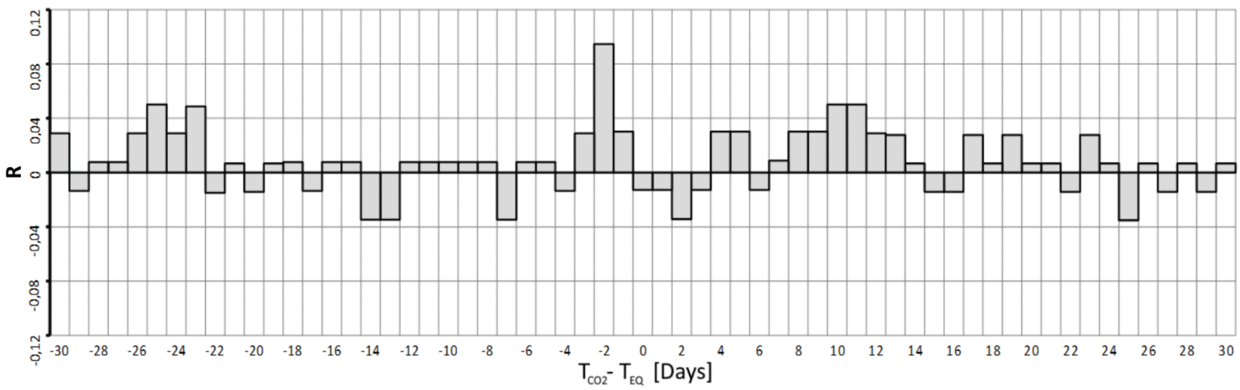

Figure SM2. Matthews correlation coefficients in the range Δt from -30 to +30 days of the time difference between CO_2 anomalies and earthquake events.

To assess the influence of low-magnitude events, we calculated an additional correlation histogram (Figure SM3) based on a reduced catalog which does not consider the M_L<2 earthquakes of Table SM2. By acting in this way, the number of significant seismic events reduced to 33. The histogram of Figure SM3 shows the correlation of these 33 earthquakes with the 61 CO_2 anomalies discussed in the main text. Despite the reduced number of events, once again, a significant correlation peak (p-value < 0.05) appears in correspondence with the time lag of -2 days, along with an additional significant peak at +11 days. The occurrence of this additional peak means that CO_2 anomalies can occur 11 days later the seismic events, when the $M_L \geq 2$.

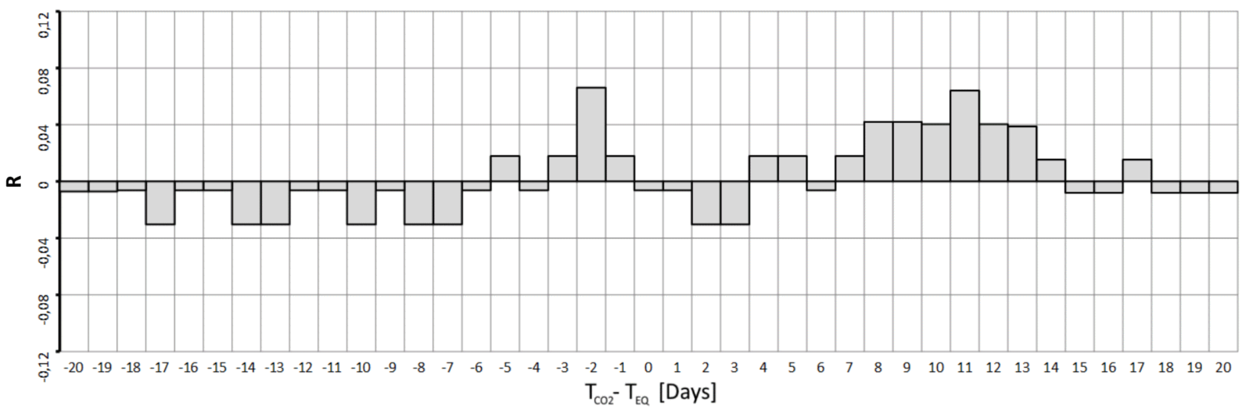

Figure SM3. Matthews correlation coefficients in the range Δt from -20 to +20 days of the time difference between CO_2 anomalies and earthquakes, calculated for a reduced earthquake dataset devoid of M_L<2 events.

We further assessed the sensitivity of the statistical method by processing a slightly revised earthquake dataset, which also includes a number of seismic events occurred within few km from the boundary of the selected area of interest (Table SM6). This exercise responded to the need to account for the uncertainty in the epicentral location (here estimated in the order of 1 to 2 km at max), which typically depends on a number of features of the seismogram pecking. Figure SM4 shows the output of this additional elaboration that considers this expanded dataset.

Table SM6. Times, coordinates, depths, and magnitudes of the 4 seismic events added to those of Table SM2 and correlated with the 61 CO_2 anomalies.

#EventID	Time	Latitude	Longitude	Depth/Km	Magnitude	Event location name	distIp	distDobr
18509381	24/03/2018	44.0872	10.8188	10.9	2.4	4 km NE San Marcello Pistoiese (PT)	32.668856	10.764652
19291171	11/05/2018	43.7777	10.308	6.4	2.4	6 km W Vecchiano (PI)	33.487934	10.764652
21994811	04/04/2019	43.8457	10.5853	7.8	2.2	1 km SE Capannori (LU)	27.712695	8.830799
25824021	21/12/2020	44.1842	10.535	9.8	1.8	7 km W Pievepelago (MO)	18.753905	5.594292

The histogram of Figure SM4 reports the correlation between the 61 selected CO_2 anomalies already discussed in the main text, and a total of 46 seismic events obtained by summing 4 "near-border" events of Table SM6 to the 42 earthquakes already considered. This histogram confirms that the same significant correlation peak at -2 days is predicted, when the maximum radius of influence is extended up to a maximum of about 2 km.

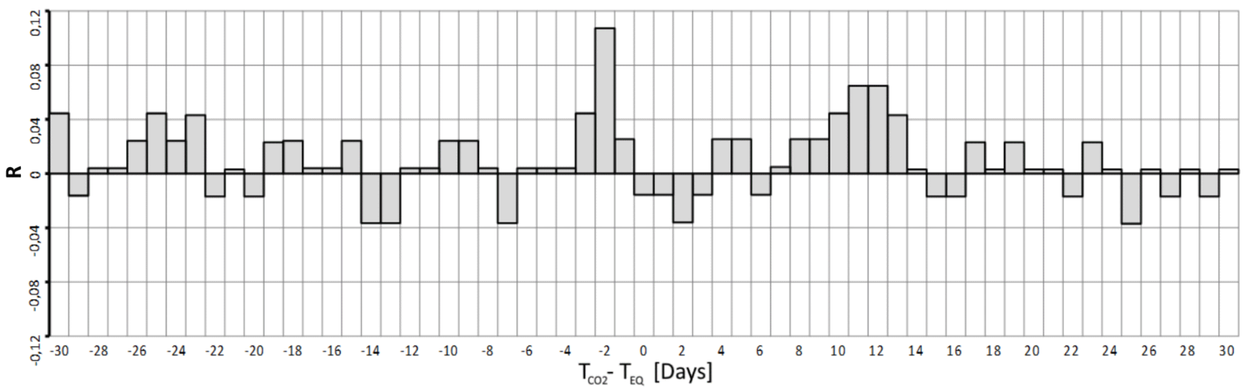

Figure SM4. Matthews correlation coefficients in the range Δt from -30 to +30 days of the time difference between CO_2 anomalies and earthquakes, calculated for an increased earthquake dataset that considers also the seismic events located within about 2 km from the border of designed zone of interest.

Overall, the findings of Figures SM2, SM3 and SM4 further corroborate the robustness of the proposed statistical approach.